

## WIDEBAND CONICAL MONOPOLE ANTENNA WITH INTEGRATED STOPBAND FILTER

Z. H. Hu<sup>\*</sup>, J. R. Kelly, P. S. Hall, and P. Gardner

School of Electronic, Electrical and Computer Engineering, University of Birmingham, Edgbaston, Birmingham, B12 2TT, UK

**Abstract**—This paper presents a conical monopole antenna with two C-shaped slots to provide a frequency stopband to suppress interference. Compared to previous work reported in the literature, the antenna provides increased gain suppression to vertically polarised signals within the notch-band of up to 41.5 dB in four specific directions. It also yields omni-directional radiation patterns at frequencies throughout the operating band, outside the rejection band. The four null directions in vertically polarised plane at the notched band frequency are explained by an analysis of simplified equivalent current sources. The effect of different length of slots has been investigated. Two methods to control the stop band directions are also discussed.

### 1. INTRODUCTION

Conical antennas are widely used both in commercial and military applications needing an omni-directional pattern and vertical polarisation [1–3]. Congestion in the spectrum is becoming a serious problem in both areas and is leading to a variety of methods to allow interoperation and to release additional resources. The underlay approach keeps transmission power below the noise level and uses wideband waveforms to communicate, such as in the ultrawide band (UWB) system. Overlay methods use higher power and search for unused spectrum, as in cognitive radio. In defense applications, conical monopole antennas are useful in observing the electromagnetic spectrum, and subsequently in jamming activity. In all these applications there is a need for stopband capabilities to reduce interference. This paper describes a conical monopole designed around the UWB/WLAN interference problem. Specifically it operates from 3.1 GHz to 10.6 GHz, and stops the

---

*Received 13 November 2011, Accepted 20 February 2012, Scheduled 27 February 2012*

\* Corresponding author: Zhen Hua Hu (zhh334@bham.ac.uk).

HIPERLAN/2 bands in Europe (5.15–5.35 GHz, 5.470–5.725 GHz) and the IEEE 802.11a band in the U.S. (5.15–5.35 GHz, 5.735–5.825 GHz). Whilst one solution to this problem is to insert a band-stop filter before the low noise amplifier (LNA) in the UWB receiver, this would increase the size, weight, and complexity of the system. An alternative solution used here is to design an antenna which incorporates an integrated band rejection filter. The antenna [4] could also be scaled to lower frequencies and used for IEEE 802.22 [5], wireless regional area network applications. Those networks would be based on cognitive radio concepts, which require a sensing antenna with an omni-directional pattern outside the stopband. The band notch would serve to protect the search receiver from saturation by high power legacy transmitters, operating in the local area.

There is a limited literature concerning UWB conical or biconical antennas with band notched behaviour. Most of designs that have been proposed are focusing on planar printed UWB antennas incorporating a notch-band [6–17]. The most widely used methods involve inserting slots into the radiating elements or the ground plane [6–14]. C shaped [6], U shaped [6–8], L shaped [9], Y-shaped [10] ring slot [11], CPW slot [12], meandered grounded stubs [13], and dual-gap open-loop slot [14] have been demonstrated. Another popular method is to use a resonator on the other side of the substrate, such as split ring resonators (SRRs) [15], square ring resonator [16], or a dual-gap open-loop resonator [14]. Parasitic elements have also been used to achieve band rejection behaviour. For example Nikolaou et al. used L shaped resonators on either side of the radiating element [17]. However, many of the proposed solutions suffer from at least one of the following limitations: 1) poor rejection at the notch frequency, 2) poor omni-directional radiation pattern at frequencies within the operating band, and are thus not suitable for IEEE 802.22 applications [5].

Hu et al. presented three dimensional monopole antennas incorporating 4 U-shaped slots [18] and 4 C-shaped slots [19] to address the limitations discussed before. The results in Ref. [18] showed that an antenna incorporating 4 U-shaped slots provides a notch band with a 6 dB return loss bandwidth of 150 MHz. This corresponds to a relatively high quality factor of 34.7. The antenna also provides 12.7 dB of peak gain suppression. The antenna incorporating 4 C-shaped slots [19] has improved band-rejection behaviour with at least 28 dB of gain suppression but with a quite low quality factor of 5.65 (with a 6 dB return loss bandwidth).

This paper presents the comprehensive study of the elliptical cone antenna with two C-shaped slots [4]. The antenna is comprised of a conical section, mounted perpendicular to the centre of a square ground

plane. The band-notch is created by cutting two slots into the surface of the cone. One of the key strengths of the antenna is that it provides very high gain suppression (about 41.5 dB) to the vertical polarization at the notch-band frequency in four specific directions of the vertical polarizations and 11.3 dB of suppression in all directions. This is a significant improvement compared to the best antennas currently available. Lui et al. [16] for example, describe an UWB slot antenna incorporating a square ring resonator, which provides about 18 dB of peak gain suppression with a relatively uncontrolled pattern at notch frequency. (Note that because peak gain suppression is not quoted explicitly in [16], the above figure is calculated from the peak direction in Fig. 5(g) in [16]).

The structure of the proposed slotted antenna and the measured results will be discussed in Section 2. Parametric study of the slotted antenna in simulations will be provided in Section 3. Section 4 describes the effect of rotating the C-shaped slots. The manufacture and fabrication process of the proposed antenna will be introduced in Section 5, and concluding remarks are made in Section 6.

## 2. STRUCTURE OF THE ANTENNA

### 2.1. Antenna Design and Structure

Figure 1 illustrates the structure of the antenna. A prototype of the antenna has been machined from solid copper, as shown in Fig. 2. Manufacturing issues are discussed in Section 5. Table 1 gives dimensions of the prototype. A second, elliptical cone antenna without slots, named as “Reference Antenna”, was also fabricated. The elliptical cone shaped antenna is inherently a wide band radiating element having an omni-directional radiation pattern [20], and is therefore well-suited for use in wideband systems [21, 22]. In this conical antenna the current is distributed evenly around the circumference, so that the slot can couple more strongly than other shapes, particularly planar types in which the current is concentrated

**Table 1.** Antenna dimensions.

$H$	20.0 mm	$g$	1.0 mm
$w_s$	0.5 mm	$r$	4.4 mm
$d$	2.0 mm	$h_f$	1.0 mm
$W_g$	40.0 mm	$t_g$	0.5 mm
$\alpha$	80°	$t_c$	0.5 mm

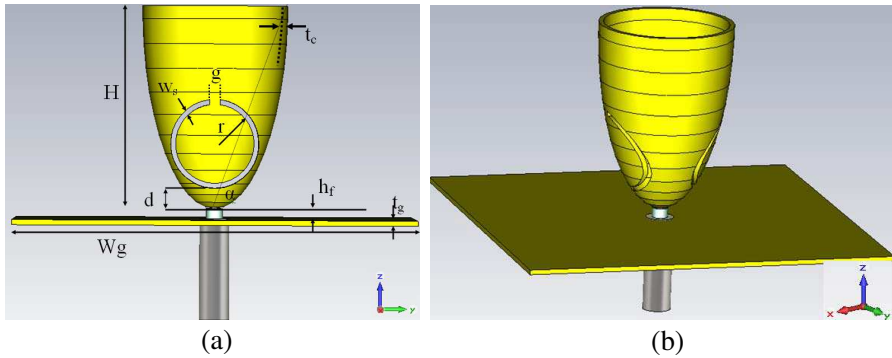


**Figure 1.** (a) Structure of elliptical cone antenna incorporating two C-shaped slots; (b) 3D view of the slotted antenna.

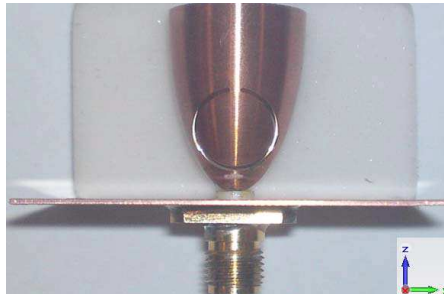


**Figure 2.** Side view of the completed fabricated prototype.

along the edge. In addition, the bottom of an elliptical cone is larger than other shapes, such as a V-shaped cone, which enables the slot to be located close to the feed-point, to further enhance coupling. The elliptical cone antenna has three parameters, namely the height of the cone, the flare angle, and the distance between the base of the cone and the ground plane. By adjusting these parameters, it is possible to optimize the antenna's radiation pattern and input impedance [21].

## 2.2. Simulation and Measurement Results

### 2.2.1. Reflection Coefficient

Simulations were performed using the transient solver in CST Microwave Studio®. Fig. 3 shows the measured return loss curves for the slotted and reference antenna. In both cases the lowest reflection coefficient is at about 10 GHz. For the simulated and measured

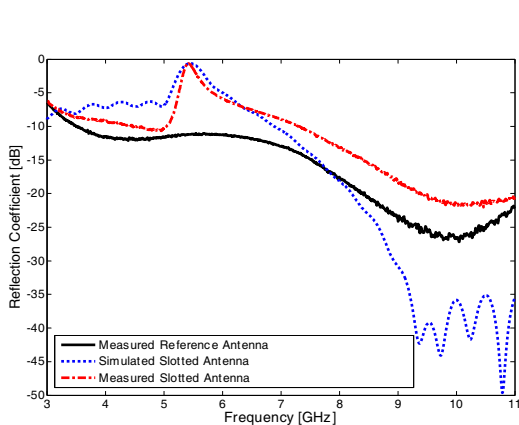


**Figure 3.** Measured reflection coefficient for reference and slotted antennas of Fig. 1

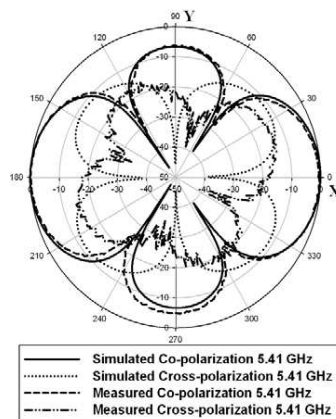


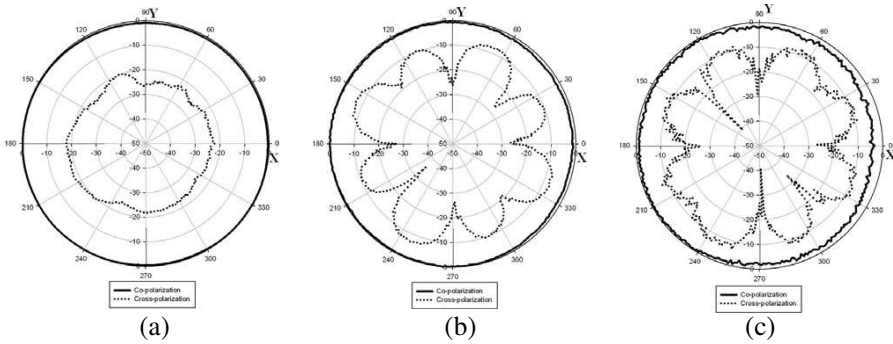
**Figure 4.** Simulated and measured normalized radiation patterns in  $H$ -( $xy$ -) plane for the antenna of Fig. 1.

antennas, the band notch is centered at 5.46 GHz and 5.42 GHz, where both values of return loss are 0.63 dB, respectively. The notch band has a 3 dB return loss bandwidth of 527 MHz and 305 MHz, respectively, which correspond to quality factors of 10.4 and 17.8. The notch demonstrated here is illustrative of what might be used to suppress either the Hiperlan/2 bands in Europe (5.15–5.35 GHz, 5.470–5.725 GHz) or the IEEE 802.11a band in the U.S. (5.15–5.35 GHz, 5.735–5.825 GHz).

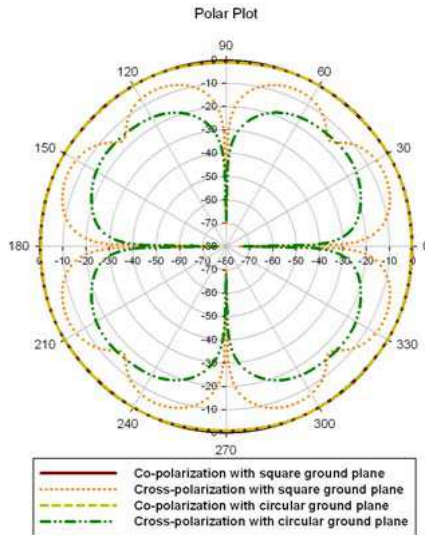
### 2.2.2. Radiation Patterns

Figure 4 shows simulated and measured radiation patterns for the antenna at 5.41 GHz in  $H$ -( $xy$ ) plane. There is a good agreement between the simulated and measured radiation patterns. The vertically polarised (co-polarisation or  $z$  directed) radiation pattern has two main lobes in the  $0^\circ$  and  $180^\circ$  positions with minor lobes in-between. The main lobes correspond to the centers of the C-shaped slots. There are also four nulls in the radiation pattern, which coincide with the sides of the slots. These nulls can be used to increase the gain suppression in the vertical polarization by placing them in the direction of known interfering signals. This would require mechanical rotation if the interference direction is dynamic, or appropriate mounting if the direction is fixed. For operation in a multipath environment,

where interference may arrive at the antenna from multiple directions, suppression will be closer to the peak pattern levels. The frequency shown in the Fig. 4 is slightly different from the notch band centre frequency, because the nulls are quite sensitive to the frequency and the deepest nulls were slightly shifted away from the centered notch frequency.



**Figure 5.** Measured normalized  $xy$ -plane radiation patterns for the antenna of Fig. 1 at: (a) 4 GHz; (b) 8 GHz; (c) 10 GHz.



**Figure 6.** Simulated normalized  $xy$ -plane radiation patterns for the antenna of Fig. 1 at 10 GHz, incorporating a  $40 \times 40 \text{ mm}^2$  square ground plane and a circular ground plane with 40 mm diameter, respectively.

The measured  $H$ -( $xy$ ) planes patterns for other frequencies are presented in Fig. 5. It is clear that the proposed antenna has an omnidirection pattern in the vertical polarisation even at high frequencies such as 10 GHz. The high cross-polarisation, shown in Fig. 5, is due to the relatively small square ground plane and can be reduced by a larger square ground plane or a circular ground. The reason for this is that the current return path for the antenna with the circular ground plane has the same length compared to the antenna with a square ground plane [23]. Fig. 6 shows the pattern comparison between the slotted antennas incorporating a  $40 \times 40 \text{ mm}^2$  square ground plane and a 40 mm diameter circular ground plane at 10 GHz. It is clear that using a circular ground can reduce the cross-polarization by at least 10 dB.

### 2.2.3. Equivalent Current Sources Study

In order to understand the origin of the pattern shape at the notch frequency, an equivalent current source model was developed. Fig. 4 shows the four nulls in the vertically polarised radiation pattern at the notched band frequency, i.e., 5.41 GHz and this pattern is repeated by the solid line in Fig. 8. The four nulls in the vertical polarisation can be explained by the location of the vertically oriented current

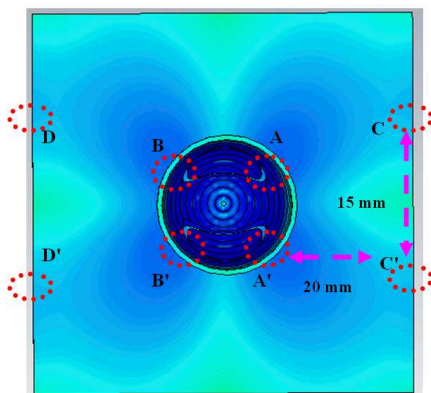


**Figure 7.** The relative locations of those current concentration on the cone and ground plane.

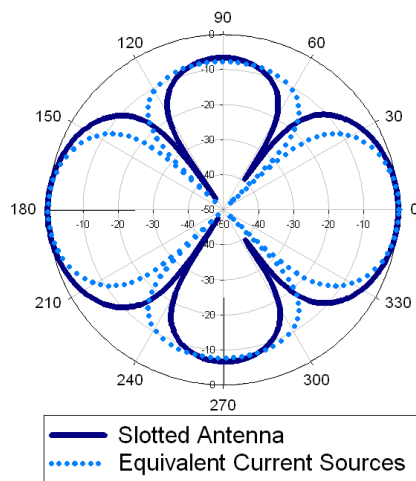


**Figure 8.** Simulated co-polarisation radiation pattern for the slotted antenna and the equivalent current sources.

concentrations around the antenna. A simulation of the surface currents on the antenna and ground plane, at 5.41 GHz, indicated that presence of strong vertical currents on the top of the slots, and on the ground plane edges, as shown in Fig. 7. To enable a first order analysis of the likely radiation pattern of these current sources, it is assumed that firstly there are strong vertical components of the currents at these locations, either across the metal bridge at the top of the C slots, or on the ground plane edge, and secondly that the currents are of equal magnitude. A simple array analysis using the equation [24] as below:

$$AF = \sum_{n=1}^N I_{1n} \left[ \sum_{m=1}^M I_{m1} e^{j(m-1)(kd_x \sin \theta \cos \phi + \beta_x)} \right] e^{j(n-1)(kd_y \sin \theta \sin \phi + \beta_y)} \quad (1)$$

in which,  $m = 2$  and  $n = 4$  in the  $x$  and  $y$  directions with distances  $dx = 15$  mm and  $dy = 20$  mm.  $\phi$  has a range from  $0^\circ$  to  $360^\circ$  and  $\theta$  is fixed at  $90^\circ$ . Both values of phase shift (i.e.,  $\beta_x$  and  $\beta_y$ ) are assumed to be  $0^\circ$ . The reasonable agreement between the array model and the full antenna shown in Fig. 8 is taken to justify this assumption. It is also assumed that the current sources have isotropic radiation patterns. Fig. 8 shows the radiation pattern of these sources derived from Equation (1), compared well to the CST simulated pattern of the slotted antenna at notched band frequency, 5.41 GHz. Several conclusions can be drawn from this simplified analysis. Firstly the deep nulls at the notch frequency are due to the interaction of sources both on the cone and ground plane. This means that changes in the ground plane may affect the null depth, and in particular the use of the cone on a very large ground plane, such as a metallic vehicle might result in reduced null depth. For example, simulation shows when using an  $80 \times 80$  mm<sup>2</sup> square ground plane, the current concentration on the ground plane get smaller. The null depth is reduced by 18 dB compared to the one with size of  $40 \times 40$  mm<sup>2</sup>. Secondly, the application of this method to horizontally polarised patterns was not immediately successful, due to the assumption of the more complex behaviour of the horizontally oriented current sources. Additional simulations indicate that the nulls become unstable or disappear if more than two C-shaped slots [19], or other shaped slots [18], are used.

#### 2.2.4. Gain Suppression

Figure 9 shows the simulated total efficiency for the reference and slotted antennas. At the operating frequency band, the total efficiency for the reference antenna is at least  $-0.7$  dB. The lowest total efficiency for the slotted antenna is  $-12.6$  dB at 5.43 GHz, which is close to

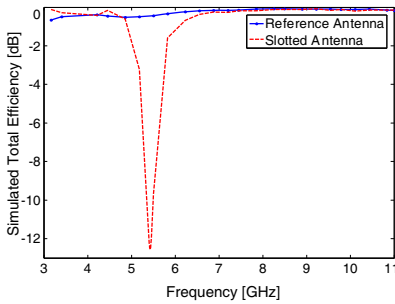


**Figure 9.** Simulated total efficiency for the slotted and reference antennas.

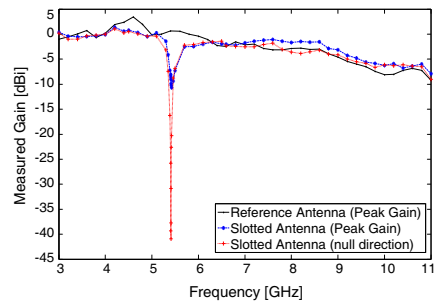


**Figure 10.** Measured vertically polarized power gain for the slotted and reference antennas in  $H$ -( $xy$ -) plane polarisation.

the simulated notch centre frequency 5.46 GHz. Such low total efficiency shows that the slotted antenna can provide good average gain suppression for the notch band in all directions. Fig. 10 shows measured power gain in dBi, in the azimuthal ( $xy$ ) plane, for the slotted and reference antenna. At the frequency of the band notch, the gain of the reference antenna is about 0.6 dBi. Such a low gain is due to the small ground plane used and the fact that the maximum directivity is not in the  $H$ -( $xy$ -) plane. In the direction of the main lobe shown in Fig. 4 ( $+x$ , or  $\phi = 0^\circ$ ), the gain is reduced to  $-10.7$  dBi, giving a gain suppression of 11.3 dB. In the direction of the lowest null (i.e.,  $\phi = 123^\circ$ ), the vertically polarised gain is  $-40.9$  dBi, giving 41.5 dB of gain suppression in the null direction.

### 3. SLOT DESIGN FOR OTHER NOTCH FREQUENCIES

The slot is approximately half-a-wavelength long at the stop band frequency, and increasing the slot length reduces the notch frequency. In order to establish whether the proposed antenna can provide good gain suppression at other frequencies, the relationship between the size of the slot and interference suppression has been studied.

To change the resonant frequency, the radius,  $r$ , of the slot is changed from 4.4 mm to  $r = 3.0$  and 5.2 mm and compared to the antenna in the previous section. Fig. 11 shows the simulated return loss for these cases. These slot sizes provide notch band centre frequencies of 4.46 GHz, 5.46 GHz and 8.04 GHz with return loss of  $-0.6$  dB,  $-0.6$  dB and  $-2.1$  dB respectively for  $r = 5.2$ , 4.4 and 3.0 mm. The notch bands have a 3 dB return loss bandwidth of 854 MHz, 527 MHz

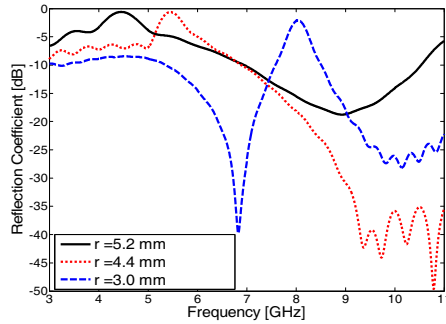


**Figure 11.** Simulated return loss for the antenna of Fig. 1 with different radius of slots, i.e.,  $r = 4.4$  mm,  $r = 5.2$  mm, and  $r = 3.0$  mm.

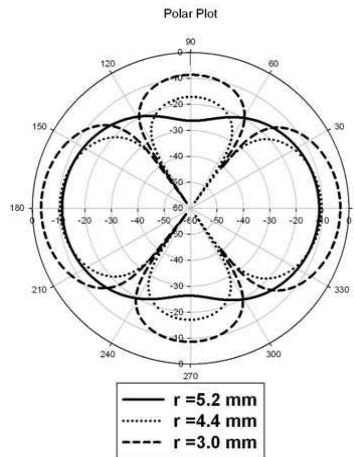


**Figure 12.** Simulated co-polarisation radiation patterns in  $H$ -( $xy$ -) plane for the antenna with different radius of C-shaped slots, i.e.,  $r = 5.2$  mm at 4.46 GHz;  $r = 4.4$  mm at 5.41 GHz; and  $r = 3.0$  mm at 8.02 GHz.

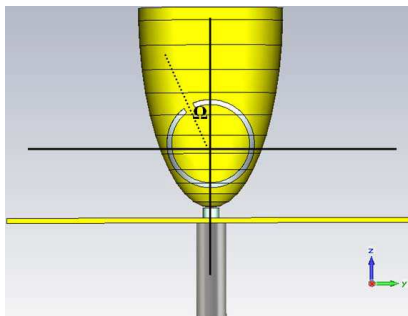
and 240 MHz respectively. These values correspond to quality factors of 5.2, 10.4 and 33.5 respectively. In each case the length of the slot is approximately half-a-wavelength at the band-notch centre frequency. The larger the radius of the C-shaped slot, the lower the notch band centre frequency and larger the quality factor.

Figure 12 shows the  $H$ -( $xy$ -) plane co-polar radiation pattern for the antenna with different slot radii at their resonant frequencies, 4.46 GHz, 5.41 GHz and 8.02 GHz respectively. The frequencies shown

in Fig. 12 are slightly different from the notch band centre frequencies shown in Fig. 11, because the nulls are quite sensitive to frequency and the deepest nulls were slightly shifted away from the centred notch frequency, as mentioned earlier. From Fig. 12, it is clear that the main lobes point in the locations of two slots while the minor lobes occur between them. The figure also shows how the slot size changes the depth of gain suppression. Although the nulls disappear when  $r = 5.2\text{mm}$ , due to the distance between current concentrations of points A and B, in Fig. 7, is getting closer, there is a significant gain suppression improvement, about 18 dB less gain, in the directions of the minor lobes (i.e.,  $\phi = 90^\circ$  and  $\phi = 270^\circ$ ). An adjustment to the shape of slot, i.e., elliptical shaped, may be possible for maintaining the four nulls in  $H$  plane.

#### 4. ANTENNA WITH ROTATED C-SHAPED SLOTS

In addition to rotation of the antenna, the notch band null directions can also be moved by changing the inclination of the slots as shown in Fig. 13. Such an inclination change could be implemented with switches located around the periphery of a continuous slot. Whilst this has not been done here, simulations are used to demonstrate the effect. Fig. 13 shows the gap in the C-shaped slot inclined to an angle of  $\Omega$  degrees. In all other respects these antennas are identical to that shown in Fig. 1(a). Six angles,  $0^\circ$ ,  $30^\circ$ ,  $45^\circ$ ,  $60^\circ$ ,  $90^\circ$  and  $180^\circ$  are simulated. Both slots are rotated in the same direction viewed from the



**Figure 13.** The structure of the elliptical cone antenna with 2 C-shaped slots and the gap shifted with an angle of  $\Omega$ .

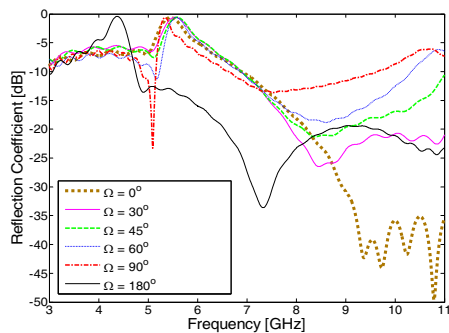


**Figure 14.** Simulated return loss curve for the structure of the elliptical cone antenna with rotated 2 C-shaped slots as shown in Fig. 13.

front of the slot. Because rotation of the slot in the opposite direction, that is  $-\Omega$ , will result in a mirror image structure to that shown in Fig. 13 and hence to patterns rotated in the opposite direction, that is  $-\Phi$ , they were not simulated. Fig. 14 shows the simulated return loss curves for each case. The notch band centre frequencies for those antennas are 5.46 GHz, 5.55 GHz, 5.58 GHz, 5.58 GHz, 5.34 GHz and 4.38 GHz, respectively. Rotating the slot from just  $\Omega = 0^\circ$  to  $90^\circ$  alters the notch band centre frequency slightly, at most 2.2% shift. However, rotation by  $180^\circ$  gives a large shift and about 19.8% change.

Figure 15 shows the simulated normalized radiation patterns in the  $H$ -( $xy$ ) plane for those antennas. From these results it is clear that rotating the C-shaped slot from  $\Omega = 0^\circ$  to  $90^\circ$  rotates the direction of the radiation pattern nulls. When  $\Omega$  is rotated from  $-90^\circ$  to  $90^\circ$  the first null can be rotated from  $\Phi = 0^\circ$  to  $87^\circ$  as shown in Table 2. Thus, as there are four nulls in the pattern one can be placed anywhere in

**Table 2.** The first null with angle  $\Phi$  in the vertical polarisation vs. rotation angle  $\Omega$ .

Rotation Angle $\Omega$	$-90^\circ$	$-60^\circ$	$-45^\circ$	$-30^\circ$	$0^\circ$	$30^\circ$	$45^\circ$	$60^\circ$	$90^\circ$
Null Angles $\Phi$	$87^\circ$	$60^\circ$	$49^\circ$	$44^\circ$	$34^\circ$	$25^\circ$	$20^\circ$	$18^\circ$	$0^\circ$

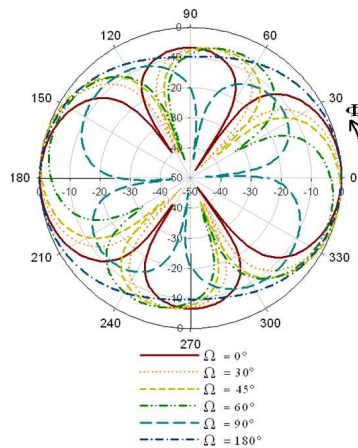


**Figure 15.** Simulated normalized radiation patterns in  $H$ -( $xy$ ) plane for the elliptical cone antenna with 2 C-shaped slots and the C-shaped slot rotates to different angular positions.

the range  $\Phi = 0^\circ$  to  $360^\circ$ . However, when the C-shaped slot is rotated to  $\Omega = 180^\circ$  the pattern becomes almost omni-directional, as shown in Fig. 15.

## 5. MANUFACTURE AND STOP BAND FREQUENCY CONTROL

The antenna was machined from solid, by first machining the outer shape from a stock copper rod, then drilling the centre hole using a CNC lathe. A small ball nose milling cutter on a CNC miller was then used to machine the internal shape of the cone. The slots were machined individually using 0.5 mm cutter with the blank cone mounted in a special fixture. Low cost production is very possible and the method used would depend on the intended frequency range. For higher frequency ranges and hence smaller size, the antennas could be die cast as is used for corrugated horns in domestic satellite dish feeds. Metallised formed plastic, as used in mobile phones could also be used. Larger size could be produced by various methods. If the cone shape is altered, albeit at the expense of bandwidth, several possibilities exist, as follows. A straight cone with circular cross section can be made by wrapping thin flexible printed circuit board or thin metal sheet with the slots formed by punching. A straight cone with square cross section can be made from four triangular printed circuit boards, as demonstrated in [25].

## 6. CONCLUSION

This paper introduces an elliptical cone antenna incorporating two C-shaped slots. Experimental results suggest that the antenna provides improved gain suppression (about 41.5 dB) in four specific directions and 11.3 dB of peak gain suppression in the vertical polarisation compared with planar antenna designs presented in the literature. Analysis of simplified equivalent current sources associated with the slot and ground plane edge currents confirms that it is indeed radiation from those sources that give rise to these well defined patterns. As expected, the band notch centre frequency can also be controlled by simply modifying the length of the C-shaped slot. The gain suppression in the null directions is affected by the distance between the C-shaped slots. If the direction of interferer changes, the antenna could be rotated mechanically. Alternatively one could effectively rotate the C-shaped slots by using a number of pin diode switches. In summary the experimental results show that the elliptical cone antenna with two C-shaped slots provides a high degree of gain reduction in

the specified direction. It will therefore be a very good candidate for suppressing interference in wideband systems that require omnidirectional patterns at the operating frequencies outside the rejection band.

## ACKNOWLEDGMENT

The authors would like to thank Mr. Zhengpeng Wang for helpful discussions and Mr. Warren Hay for workshop support at the University of Birmingham.

## REFERENCES

1. Palud, S., F. Colombel, M. Himdi, and C. Le Meins, "Compact multi-octave conical antenna," *Electronics Letters*, Vol. 44, 659–661, 2008.
2. Wei, C. and Z. Shen, "Design of a compact and broadband conical monopole antenna," *IEEE Antennas and Propagation Society International Symposium, APSURSI'09*, 1–4, Jun. 2009.
3. Palud, S., F. Colobel, M. Himdi, and C. Le Meins, "A novel broadband eighth-wave conical antenna," *IEEE Transactions on Antennas and Propagation*, Vol. 56, 2112–2116, 2008.
4. Hu, Z. H., P. S. Hall, J. R. Kelly, and P. Gardner, "Wideband conical monopole antenna with frequency band notched behaviour," *Electronics Letters*, Vol. 46, No. 23, 1542–1543, 2010.
5. IEEE 802.22 Wireless Regional Area Networks — Enabling Rural Broadband Wireless Access Using Cognitive Radio Technology, IEEE 802.22-10/0073r03, Jun. 15, 2010.
6. Nikolaou, S., B. Kim, Y.-S. Kim, J. Papapolymerou, and M. M. Tentzeris, "CPW-fed ultra wideband (UWB) monopoles with band rejection characteristic on ultra thin organic substrate," *Proceedings of APMC 2006*, CD-Rom: FROF-26, Dec. 12–15, 2006.
7. Antonino-Daviu, E., M. Cabedo-Fabres, M. Ferrando-Bataller, and A. Vila-Jimenez, "Active UWB antenna with tunable band-notched behaviour," *Electronics Letters*, Vol. 43, No. 18, 959–960, 2007.
8. Zheng, Z.-A. and Q.-X. Chu, "A CPW-fed ultrawideband antenna with dual notched bands," *IEEE International Conference on Ultra-wideband, ICUWB 2009*, 645–648, 2009.

9. Pancera, E., D. Modotto, A. Locatelli, F. M. Pigozzo, and C. de Angelis, "Novel design of UWB antenna with band-notch capability," *European Conference on Wireless Technologies*, 48–50, 2007.
10. Jiang, J.-B., Z.-H. Yan, and C. Wang, "A novel compact UWB notch-filter antenna with a dual-Y-shaped slot," *Progress In Electromagnetics Research Letters*, Vol. 14, 165–170, 2010.
11. Zhang, Y., W. Hong, C. Yu, Z.-Q. Kuai, Y.-D. Don, and J.-Y. Zhou, "Planar ultrawideband antennas with multiple notched bands based on etched slots on the patch and/or split ring resonators on the feed line," *IEEE Transactions on Antennas and Propagation*, Vol. 56, No. 9, 3063–3068, 2008.
12. Weng, Y. F., W. S. Cheung, and T. I. Yuk, "Ultrawideband antenna using CPW resonators for dual-band notched characteristic," *International Conference on Wireless Communications & Signal Processing*, 1–4, 2009.
13. Weng, Y. F., W. J. Lu, S. W. Cheung, and T. I. Yuk, "UWB antenna with single or dual band-notched characteristic for WLAN band using meandered ground stubs," *Antennas & Propagation Conference*, 757–760, Loughborough, UK, 2009.
14. Kelly, J., P. S. Hall, and P. Gardner, "Planar band-notched UWB antenna," *3rd European Conference on Antennas and Propagation*, 1636–1639, 2009.
15. Ghatak, R., R. Debnath, D. R. Poddar, P. K. Mishra, and S. Chaudhuri, "A CPW fed planar monopole band notched UWB antenna with embedded split ring resonators," *Antennas & Propagation Conference*, 645–647, Loughborough, UK, 2009.
16. Lui, W.-J., C.-H. Cheng, and H.-B. Zhu, "Improved frequency notched ultrawideband slot antenna using square ring resonator," *IEEE Antennas and Propag.*, Vol. 55, No. 9, 2445–2450, 2007.
17. Nikolaou, S., A. Amadjikpe, J. Papapolymerou, and M. M. Tentzeris, "Compact ultra wideband (UWB) elliptical monopole with potentially reconfigurable band rejection characteristic," *Proceedings of APMC*, 1–4, 2007.
18. Hu, Z. H., P. S. Hall, J. R. Kelly, and P. Gardner, "Wideband omni conical monopole antenna with high  $Q$  band-notched behaviour," *The International Workshop on Antenna Technology*, 37–40, 2011.
19. Hu, Z. H., P. S. Hall, J. R. Kelly, and P. Gardner, "Improved band-notched wideband conical monopole antenna," *Microwave and Optical Technology Letters*, Vol. 53, No. 8, 1825–1829, May 17, 2011.

20. Kawakami, H. and G. Sato, "Broad-band characteristics of rotationally symmetric antennas and thin wire constructs," *IEEE Transactions on Antennas and Propagation*, Vol. 35, No. 1, 26–32, Jan. 1987.
21. Jamali, J., N. Tayarzade, and R. Moini, "Analyzing of conical antenna as an ultra-wideband antenna using finite difference time domain method," *International Conference on Electromagnetics in Advanced Applications*, 994–997, 2007.
22. Adachi, S., R. Kouyoumjian, and R. van Sickle, "The finite conical antenna," *IRE Transactions on Antennas and Propagation*, Vol. 7, 406–411, 1959.
23. Arai, H., *Measurement of Mobile Antenna Systems*, 42–43, Artech House, 2001, ISBN 1-58053-065-6.
24. Balanis, C. A., *Antenna Theory: Analysis and Design*, 3rd edition, 349–362, John Wiley & Sons, 2005.
25. Hu, Z. H., P. S. Hall, J. R. Kelly, and P. Gardner, "UWB pyramidal monopole antenna with wide tunable band-notched behaviour," *Electronic Letters*, Vol. 46, No. 24, 1588–1590, 2010.